



FEATURE ARTICLE

# Parasitic infection of the diatom *Guinardia delicatula*, a recurrent and ecologically important phenomenon on the New England Shelf

Emily E. Peacock, Robert J. Olson, Heidi M. Sosik\*

Biology Department, Woods Hole Oceanographic Institution, Woods Hole, Massachusetts 02543, USA

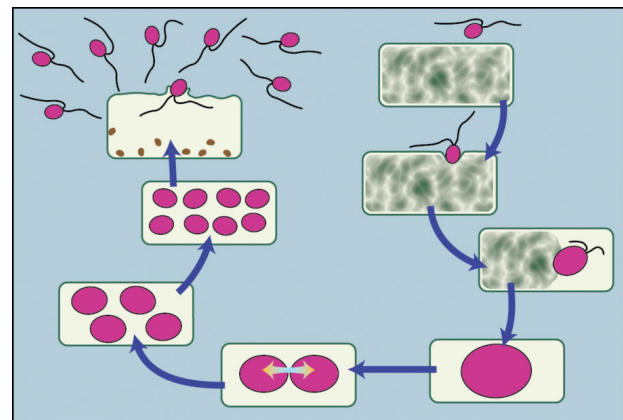
**ABSTRACT:** Plankton images collected by Imaging FlowCytobot from 2006 to 2013 at the Martha's Vineyard Coastal Observatory (Massachusetts, USA) were used to identify and quantify the occurrence of the diatom *Guinardia delicatula* and of a parasite that seems specific to this host. We observed infection with morphological stages that appear similar to the parasite *Cryothecomonas aestivalis*. Our results show that events during which infection rates exceed 10% are recurrent on the New England Shelf and suggest that the parasites are an important source of host mortality. We document a significant negative relationship between bloom magnitude and parasite infection rate, supporting the hypothesis that the parasites play a major role in controlling blooms. While *G. delicatula* is observed during all seasons, the infecting stages of the parasite are abundant only when water temperature is above 4°C. The anomalously warm water and small *G. delicatula* bloom during the winter of 2012 provided evidence that parasites can be active through winter if temperatures remain relatively high. As climate change continues, winter periods of water below 4°C may shorten or disappear in this region, suggesting that parasite effects on species such as *G. delicatula* may increase, with immediate impacts on their population dynamics.

**KEY WORDS:** Phytoplankton · Diatom · Parasite · Imaging flow cytometry · MVCO · *Guinardia delicatula* · *Cryothecomonas aestivalis*

Resale or republication not permitted without written consent of the publisher

## INTRODUCTION

Parasites of phytoplankton are potentially influential drivers of phytoplankton bloom dynamics, but concrete, quantitative evidence is difficult to acquire.



Nanoflagellate parasites that consume cytoplasm and reproduce inside diatom host cells have important impacts on coastal blooms.

Image: Jack Cook (WHOI)

While the idea has been recognized for decades (Canter & Lund 1948), limited spatial–temporal resolution associated with traditional sampling techniques makes it challenging to observe population effects of parasites adequately, and sample preservation often prevents identification of parasite species. Parasites and pathogens that are known to impact a wide variety of phytoplankton hosts include viruses documented to restrict or terminate *Phaeocystis* blooms (Brussaard et al. 2005), fungi that can influence bloom dynamics and succession in diatoms (Ibelings et al. 2011, Sime-Ngando 2012), dinoflagellates that infect other dinoflagellates (Coats & Park 2002, Chambouvet et al. 2008), and bacteria that infect dinoflagellates and may be useful for toxic bloom control (Kim et al. 2008). Most knowledge of

\*Corresponding author: hsosik@whoi.edu

the biology of diatom parasites has come from investigation of isolates in culture (Drebes & Schnepf 1982, 1988, 1998, Schnepf et al. 1990, Drebes et al. 1996, Kühn et al. 1996). In contrast to the view that diatoms are typically grazed by macrozooplankton, these studies identified and described organisms that consume diatoms but are just a fraction of the size of the diatoms themselves. All parasites complete part of their life cycle in or on their host; while typical parasites do not kill their hosts, these diatom studies documented lethal parasites or parasitoids that actually consume host cells during their development. Tillmann et al. (1999) were able to extend this culture work to show that in a natural system, diatom losses associated with these parasitoids can be important. They were able to document and quantify an intensive infection of *Guinardia delicatula* and *G. flaccida* by several parasites in German coastal waters. Substantial investment in expert taxonomy and manual microscopy was required to reach these findings. Because few research programs can meet these demands, our knowledge of how widespread and recurrent these types of phenomena may be in a range of natural waters has remained limited.

New observational approaches have the potential to address some of these limitations. Molecular analyses that can be used to identify and quantify hosts, parasites, and pathogens (including fungi, viruses, bacteria, or protists) are an important avenue forward (Chambouvet et al. 2008, Gachon et al. 2010). While the potential of automated *in situ* genetic characterization exists (Scholin et al. 2006), at present these kinds of analyses still typically suffer from the limitations associated with discrete sampling. Automated imaging-in-flow cytometry (Sieracki et al. 1998, Olson & Sosik 2007, Sosik & Olson 2007) offers a complementary approach. While the cell images produced with these approaches cannot provide the taxonomic detail and definitive identification possible with molecular characterization of parasites, they have potential to meet needs for temporally and spatially resolved studies of natural populations of interacting hosts and parasites.

Time series observations with instruments that combine flow cytometry and microscopy can provide new insights into many aspects of community dynamics in natural systems. Because it is fully automated, submersible, and resistant to bio-fouling, Imaging FlowCytobot (IFCB; Olson & Sosik 2007) can be deployed for 6 mo or longer without maintenance and is now providing time series observations at a number of coastal locations (Campbell et al. 2010, 2013, Sosik et al. 2010, Brosnahan et al. 2013). The

longest of these time series is underway at the Martha's Vineyard Coastal Observatory (MVCO) on the New England Shelf. IFCB was first deployed at MVCO in June of 2006 and since then has been almost continuously collecting images of phytoplankton and other particles in the size range ~5 to 150  $\mu\text{m}$ . At MVCO, IFCB is deployed side-by-side with FlowCytobot (FCB; Olson et al. 2003), which is optimized to analyze picoplankton and small nanoplankton (~1 to 10  $\mu\text{m}$ ). Together the 2 instruments generate an unprecedented, continuous and high-resolution phytoplankton time series that offers capabilities not feasible with traditional microscopy and discrete samples (Sosik et al. 2010). This time series provides insights into life cycles and growth patterns of picocyanobacteria, diatoms, dinoflagellates, other types of phytoplankton, and some types of protozoa (e.g. herbivorous or mixotrophic ciliates). The vast quantity of images in this multi-year time series provides an exceptional opportunity to characterize the occurrence of different types of plankton–plankton interactions, including parasites of phytoplankton.

Here we present details of interactions between the centric diatom *G. delicatula* and a nanoflagellate parasite/parasitoid similar to *Cryothecomonas aestivalis* as described by Drebes et al. (1996), and their recurring interactions as documented by IFCB throughout the time series from June 2006 to September 2013. While many species are present in the MVCO time series and blooms are typically multi-species events, *G. delicatula* represents one of the greatest contributors to phytoplankton biomass, which is also true in another temperate coastal time series (Schlüter et al. 2012). From an ecological perspective, major questions persist concerning the factors that promote diatom bloom events and determine how long a bloom lasts. Schlüter et al. (2012) have recorded 45 yr of *G. delicatula* blooms showing a predominantly summer bloom with decadal scale changes in duration and timing of onset; in our shorter time series, we also see some variation, but with a predominantly winter bloom. The nanoflagellate parasite of *G. delicatula* is recognizable throughout our data set during 2 of its presumed 3 life stages due to the distinct morphology within *G. delicatula* frustules during infection. Our results indicate that the parasite commonly contributes to the decline of *G. delicatula* blooms. This finding suggests that diatom parasites may be more prevalent than previously considered and presents quantitative evidence of parasite attacks as an important influence on the fluctuation of a prominent diatom species in coastal temperate waters.

## MATERIALS AND METHODS

### Study site

MVCO is a cabled facility located off the south shore of the island of Martha's Vineyard (Massachusetts, USA), which provides shore-based power and high speed 2-way communications to an undersea node at a depth of 12 m, and to a tower structure 3 km offshore in 15 m water depth (Austin et al. 2000, Fredericks et al. 2006). The offshore tower is located at 41° 19.5' N, 70° 34.0' W and this is where IFCB has been repeatedly deployed at a depth of 4 m below mean water level, with water sampling conducted at the instrument depth. Deployments between 2006 and 2009 were conducted with a single instrument, with some extended gaps during maintenance periods. Beginning in 2010, 2 instruments were available, providing the capability for same-day turnaround and much reduced data gaps. In total, data were collected from 20 IFCB deployments ranging from 3 to 350 d (mean 120 d after 2006) from 2006 through 2013. Core measurements at the MVCO facility provide a broad suite of publicly available meteorological and hydrographic data ([www.whoi.edu/mvco](http://www.whoi.edu/mvco)), including temperature (Sea-Bird Electronics, MicroCAT) measured at the undersea node, which is located approximately 1.5 km from the offshore tower. Temperature measurements (Sea-Bird Electronics, MicroCAT) were also made during most of the time period at the same depth (4 m) and location (offshore tower) as IFCB sampling.

### IFCB

Details of the IFCB instrument and data collection have been described previously (Olson & Sosik 2007). Briefly, IFCB uses a combination of video and laser-based flow cytometric technology to both capture images of nano- and microplankton and measure their chlorophyll fluorescence. The images obtained with IFCB are of high enough resolution (~1 µm) that many plankton taxa can be recognized to genus or even species (Sosik & Olson 2007). Particles can be analyzed at rates up to 12 Hz, and observed particle concentrations typically produce on the order of 10 000 fluorescence-triggered events h<sup>-1</sup> during deployments at MVCO. IFCB was configured to analyze a new 5 ml sample of seawater approximately every 20 min. Since IFCB uses fluorescence triggering for image capture, a high proportion of the stored images contain phytoplankton cells, colonies,

or chains. Real-time image analysis on IFCB is used to segment images, and only regions of interest (portions of the camera field that contain a target) are stored for subsequent analysis. The full data set of IFCB images is accessible at <http://ifcb-data.whoi.edu/mvco>. We have shown previously that the IFCB imaging approach provides similar results to enumeration with traditional manual microscopy for a variety of phytoplankton species including *Guinardia delicatula* (Olson & Sosik 2007).

### Data analysis

Our routine analysis of the image data set starts with automated image processing and classification following the approach described by Sosik & Olson (2007), with the modification that we currently use an assemblage of decision trees constructed following the random forest approach of Breiman (2001) in place of the support vector machine described previously. The current automated classifier has 50 categories, including 28 diatom genera or species (including *G. delicatula*), as well as dinoflagellate taxa, miscellaneous nanoplankton, ciliate taxa, and detritus. We have previously shown that this automated classification approach is highly accurate (>90% correct identifications) for many diatom taxa including *G. delicatula* (Olson & Sosik 2007). While the requirement for taxonomic expertise to define the classes of interest is similar to that needed for manual microscopy, the image archive provides infinite flexibility to adjust and refine classifications in response to new information or applications; this can be done long after the sampling and initial analysis is complete. The approach also allows reanalysis or more detailed retrospective analysis as topics of interest emerge. Subsequent to automated classification, we take advantage of this flexibility to conduct routine computer-assisted manual verification and correction of approximately 3 h of observations from each month, selected such that there is at least one verified time point for each 2 wk interval throughout the time series. In this verification step, we resolve errors made by the automated classifier and subdivide selected categories into more finely resolved groups. The manually corrected 3 h of data represent ~30 ml of water, and contain anywhere from 5000 to 100 000 images of phytoplankton, detritus, and microzooplankton. As part of this step, for the *G. delicatula* category, cells and chains with visible signs of internal parasite infection were manually annotated. As described by Drebes et al. (1996), the first life cycle stage of the parasite is a motile, colorless

flagellate, either outside the host or inside the host before food uptake. Free cells of this stage are not likely to be imaged by IFCB since they do not contain chlorophyll (though they may have sometimes been included in a *G. delicatula* image, e.g. Fig. 1a). Neither these free swimming flagellates nor small attached cells have distinctive enough morphology to be certain about their identity as parasites; therefore they were not considered in this analysis.

For this study, some additional manual classification was carried out focused only on *G. delicatula* and *G. delicatula* with parasites to increase resolution during parasite events discovered during the routine analyses. For further analyses, concentrations in each category are presented after daily binning (i.e. sum of observed counts in all 20 min time points divided by total volume of seawater analyzed in the time points during a single day). Only time points that were manually verified (after initial automated classification) were included in these daily binned estimates and presented in this study. Misclassification errors associated with the automated analysis were removed from all results presented and discussed below. Whether by automated or manual classification, each count in our data set represents one region of interest or image. An image may have a single cell, or a long chain or colony of cells, depending on the species. To constrain biomass contributions, we conduct further automated analysis to estimate the biovolume of cells in the images following the approach described by Moberg & Sosik (2012), and then estimate carbon content from biovolume following the relationships determined by Menden-Deuer & Lessard (2000) from meta-analysis of extensive culture studies. For the purpose of characterizing infection, however, any image containing even one cell of parasite attack was counted as infected. This might be a single cell, a long chain with one cell attacked, or a long chain with multiple attacks.

Distinct bloom events for *G. delicatula* were identified on the basis of chain concentration. We defined important events according to contiguous periods when daily-binned concentration exceeded 2 chains  $\text{ml}^{-1}$  and the peak was at least 5 chains  $\text{ml}^{-1}$ . This analysis resulted in 12 identified events over the entire time series. Three events during 2008 occurred during periods with data gaps such that the events are incompletely characterized, so these were excluded from subsequent analyses. For each event, total bloom magnitude ( $B$ ) was computed by integrating (trapezoidal method) time-dependent abundance ( $C(t)$ ) from the time that daily concentration first

exceeded 2  $\text{ml}^{-1}$  ( $t_{\text{start}}$ ) until it dropped below that concentration again and stayed below for at least 1 wk ( $t_{\text{end}}$ ):

$$B = \int_{t_{\text{start}}}^{t_{\text{end}}} C(t) dt \quad (1)$$

The correlation coefficient ( $r$ ) between bloom magnitude and infection rate (average during each event) was computed to determine the amount of variance explained ( $r^2$ ). We tested for significance of a negative relationship between these quantities with a 1-tailed  $t$ -test. We tested for outliers in this relationship with a 2-tailed  $t$ -test applied to externally Studentized residuals (i.e. each residual divided by the standard deviation estimated with that point excluded) from the least squares linear regression.

## RESULTS

During routine manual classification of IFCB images, we observed *Guinardia delicatula* chains with unusual cytoplasm and chloroplast morphology in some cells, while other cells in the same chain looked normal. Upon closer examination of the affected chains, we observed what appeared to be the second and third parasitic stages of *Cryptothecomonas aestivalis* as described by Drebes et al. (1996; Fig. 1b–k). The second stage, in which a trophont stage of the parasite gradually phagocytizes the diatom protoplast (Drebes et al. 1996), is readily visible in IFCB images (Fig. 1b,c). The third stage, digestion accompanied by cell division, is the most commonly found stage in the images (Fig. 1d–k). Initially, one flagellate consumes all of the protoplast within a cell (Fig. 1d,e) and then produces 2, 4, 8, or more daughter cells (Fig. 1f–k). Multiple infections are also possible within one *G. delicatula* chain (Fig. 1j,k). Previous parasitic attack (completed when the parasite offspring exit the frustule) is evident when empty frustules contain fecal remains that were excreted from the parasite before the last cell division (Drebes et al. 1996; Fig. 1k). In culture studies of *C. aestivalis*, the entire vegetative life cycle took 18 to 20 h (Drebes et al. 1996). Since higher-resolution microscopy or genetic analysis would be required to confirm the identity of the parasites in this study, we can conclude only that the parasites we observed are similar to *C. aestivalis* in appearance, lifecycle, and host. We focus the rest of the analysis on how they affect the bloom dynamics of *G. delicatula* in our study area and consideration of the conditions that may control parasite impact.

Seven years of image data from mid-2006 to late 2013 show a winter bloom of *G. delicatula* every year, usually starting after 1 January and peaking in February or March (Fig. 2a,b). In addition, most years have an occurrence of *G. delicatula* in the summer or fall, which is usually (but not always) smaller than the winter blooms. The parasite of *G. delicatula* (which we detect only when *G. delicatula* is present), is abundant during many but not all of the blooms (Fig. 2c). There are repeated occurrences when infected chains represent greater than 10% of the observed *G. delicatula* population (Fig. 2b), and infection rates sometimes exceed 30% (Fig. 3).

Average daily water temperature from the area ranged from  $-0.16^{\circ}\text{C}$  in the coldest winter (2009) to

$21.5^{\circ}\text{C}$  in the warmest summer (2012) (Fig. 2d). The winter of 2011–2012 represents an anomaly, only dropping to  $3.6^{\circ}\text{C}$ , while the next warmest winter was 2007–2008, with a temperature minimum of  $1.9^{\circ}\text{C}$ . The data set spans substantive inter-annual variability in both the arrival date and the duration of cold ( $<4^{\circ}\text{C}$ ) water in winter (Fig. 2d). While there is some temperature stratification in summer and early fall ( $\sim 0.5\text{--}1^{\circ}\text{C}$ ), temperature patterns are very similar between 4 m observations near IFCB and bottom depth (12 m node) observations. We used the bottom record for further analyses and comparison to IFCB observations because it is more complete across the full study time period.

## DISCUSSION

Parasitic interactions in the phytoplankton may be common and varied (Van Donk 1989, Coats & Park 2002, Park et al. 2004, Montagnes et al. 2008, Gachon et al. 2010, Ibelings et al. 2011), but they have been difficult to study in a quantitative manner in natural systems. We have taken advantage of a cabled observatory facility (MVCO) to carry out extended time series observations with IFCB of a particular parasite–host relationship in waters of the New England Shelf. The diatom host, *Guinardia delicatula*, is a recurrent and important contributor to total phytoplankton biomass in this system (Fig. 2a,b). While we cannot be certain about the identity of the parasite observed in our time series, it exhibits characteristics that are entirely consistent with morphological and life cycle properties described for *Cryothecomonas aestivalis* by Drebes et al. (1996). Interestingly, while *G. delicatula* always occurs in mixed assemblages that include a number of other diatom taxa, we almost never observed this or any similar parasite in association with other diatoms even when the rate of infection in *G. delicatula* was very high, the only exception being very rare instances of possible infection in other species of the same genus, viz. *G. flaccida* and *G. striata*. This level of specificity in the parasite–host relationship echoes findings of Tillmann et al. (1999) in the North Sea and culture work of Drebes et al. (1996).

Our extended time series shows definitively that parasite infection is a recurrent feature of *G. delicatula* blooms, and further suggests that infection is ecologically important. Infection rates exceeding 10% occur in every year of the record, most commonly in late fall or early winter, but also sometimes in summer (Fig. 2b). While previous studies did not address

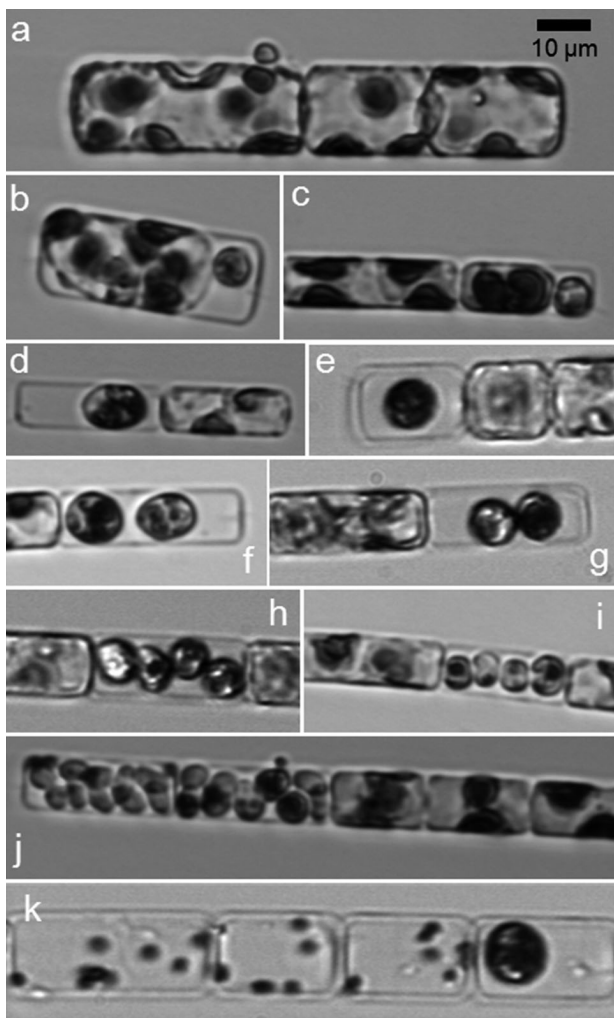


Fig. 1. Imaging FlowCytobot images of the parasite stages during infection of *Guinardia delicatula*: (a) possible external flagellate; (b,c) trophont initiates consumption of protoplast; (d,e) trophont at the end of nutritive phase; (f,g) 2 parasite daughter cells after first cell division; (h,i) 4 daughter cells; (j) 8 or more daughter cells; (k) empty frustules containing fecal remains

multi-year recurrence, the high infection rates and aspects of the seasonality we observe are consistent with reports from the North Sea (Drebes et al. 1996, Tillmann et al. 1999). Since the parasite life cycle is likely to be complete in less than 24 h and results in complete loss of the host cell (Drebes et al. 1996), multi-day events with infection rates as high as 10 to 30% strongly support the idea that this is a source of host mortality that can rival that of zooplankton grazing.

We further examined our data set to investigate what conditions are favorable to the presence of the parasite and what effect the parasites may have on *G. delicatula* population dynamics. We identified 9 events of high parasite infection (>2 d with >10% of

*G. delicatula* chains infected). Notably, the largest-amplitude *G. delicatula* blooms (i.e. late winter 2010, 2011, and 2013) occurred at times when parasites were minimal or absent (Fig. 2). While there were occasional observations of parasites when the water was colder than 4°C (Figs. 2 & 3), all of the parasite events began when temperature was above 4°C. The few cases when parasites persisted after water temperature dropped below 4°C appeared to be associated with earlier high rates of infection and periods when temperatures lingered just below or fluctuated around 4°C (Fig. 2, see also Fig. 3b,d,i).

The high infection rate events reveal a variety of scenarios, depending on whether *G. delicatula* was already established when the parasites appeared

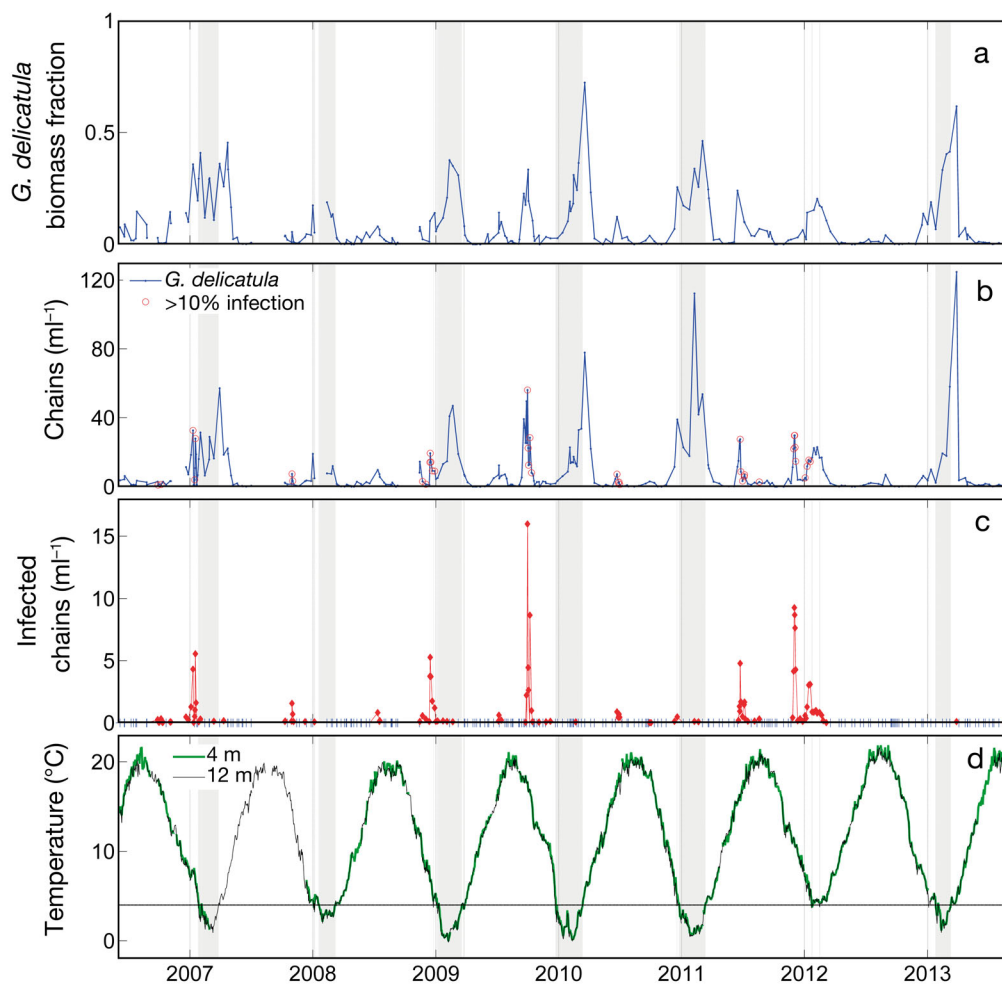


Fig. 2. Multi-year time series at Martha's Vineyard Coastal Observatory, with grey bars highlighting time periods when water temperature was <4°C. (a) *Guinardia delicatula* as a fraction of total phytoplankton biomass (considering cells with equivalent spherical diameter >10 µm). (b) Abundance of *G. delicatula* chains; red circles indicate days with >10% of chains containing at least 1 infected cell. (c) Occurrence of *G. delicatula* chains containing parasites or fecal remains; filled red diamonds indicate presence of parasites and blue ticks mark days that were manually inspected, but no parasites were found. (d) Water temperature at 4 and 12 m depths, with horizontal line at 4°C. In all panels, the absence of lines connecting adjacent data points indicates gaps of 30 d or longer in the observational records

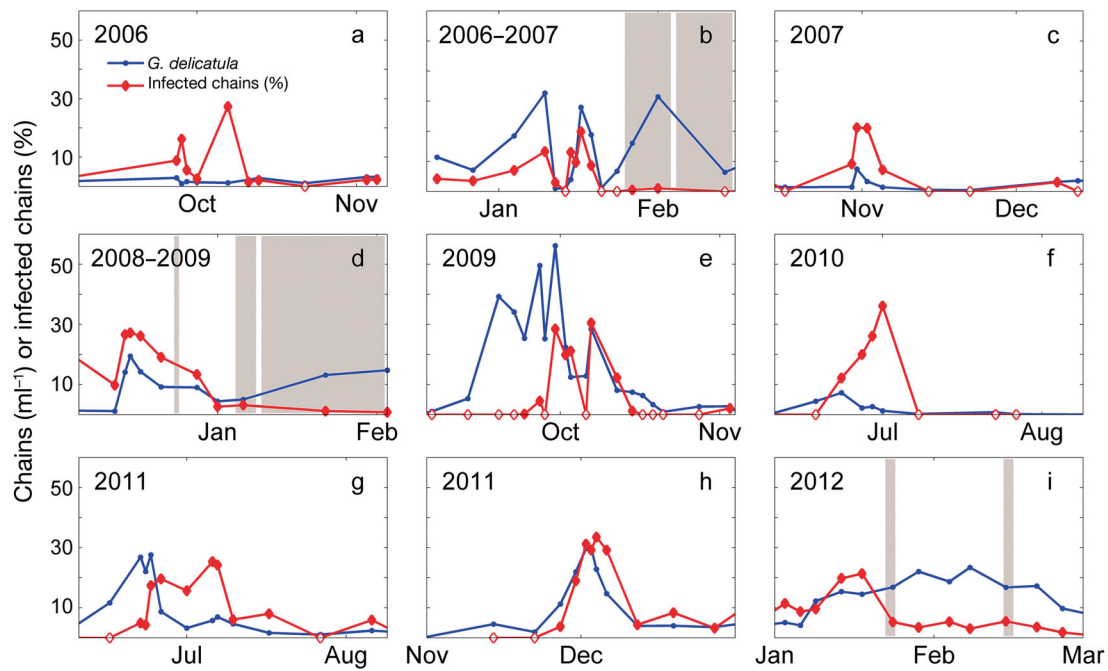


Fig. 3. Two-month time series highlighting events of high parasite infection (>2 d with >10% of *Guinardia delicatula* chains infected). Grey regions highlight time periods when water temperature was <4°C. Blue lines indicate the number of *G. delicatula* chains ml<sup>-1</sup>. Filled red diamonds indicate days with detected parasite presence, while empty red diamonds mark days when images were manually inspected for parasites, but none were found

and on the water temperature during the event (Fig. 3). In all 3 cases of parasite attack in early winter, when the water temperature dropped below 4°C the parasites declined while *G. delicatula* increased (Fig. 3b,d,i). December 2008 (Fig. 3d) and winter 2012 (Fig. 3i) are cases where the water temperature hovered around 4°C. In 2008, the parasites persisted through the beginning of winter, and then declined when the water reached more typical winter temperatures. In 2012, when water temperature barely dipped below 4°C, the parasites were present for the entire season (Fig. 3i).

The remaining parasite scenarios all occurred while the water was well above 4°C. On several occasions *G. delicatula* was fairly well established in the summer or fall and then declined with the onset of parasite attack (Fig. 3e,g). For example, in October 2009, the concentration of *G. delicatula* reached levels often seen during winter blooms. After a few weeks, the number of chains infected with parasites also increased and then the *G. delicatula* population plummeted (Fig. 3e). At other times, parasites were observed nearly simultaneously with the first host cells and the event was small and brief (Fig. 3a,c,f). Late in 2011, the *G. delicatula* winter bloom appeared to get an early start, only to be curtailed by parasite infection (Fig. 3h). Once host levels dropped

below 10 chains ml<sup>-1</sup>, infection rates dropped dramatically and the host maintained low levels until a second modest bloom was able to take hold and persist for 2 mo in early 2012 (Fig. 3i).

The infection patterns we observed in the time series strongly suggest a role for temperature in regulating parasite occurrence. It is expected that high infection rates cannot occur unless host abundances are elevated, but this is apparently not a sufficient condition for infection since many periods of high host abundance have little or no infection (Fig. 2). The highest infection rates we observed were ~30% of *G. delicatula* chains (at least one infected cell). These high rates occurred when hosts chains were present at >2 ml<sup>-1</sup> and usually >5 ml<sup>-1</sup>. Notably, they also always occurred when water temperature was >4°C (Fig. 4). Low or undetectable presence of parasites during warmer periods was typically associated with low host abundance (i.e. points near the x-axis in Fig. 4 tend to have a low host concentration when T > 4°C). Furthermore, when the water was colder than 4°C, infection rate rarely exceeded 2%, despite many times with plentiful hosts. Taken together, these results lead us to the hypothesis that the parasite is inhibited by low temperatures, with the corollary that cold conditions favor host blooms that can increase to high abundance and persist for long periods in the ab-

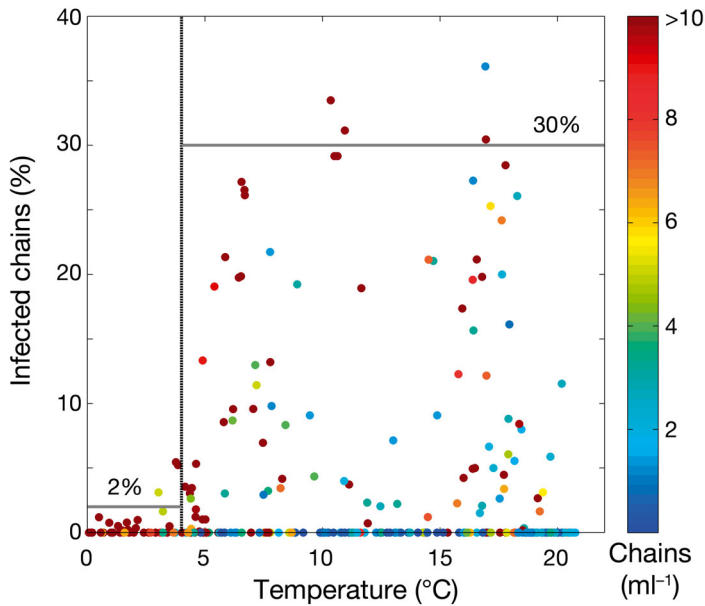


Fig. 4. Relationship between *Guinardia delicatula* infection and water temperature (°C). Color scale for symbols indicates total *G. delicatula* abundance (chains ml<sup>-1</sup>). Note that all values greater than 10 chains ml<sup>-1</sup> appear dark red (overall range extends to ~120 chains ml<sup>-1</sup>; see Fig. 2). Dashed vertical line marks 4°C, horizontal lines mark infection rates of 2 and 30%. Note that the highest infection rates only occur at temperatures >4°C

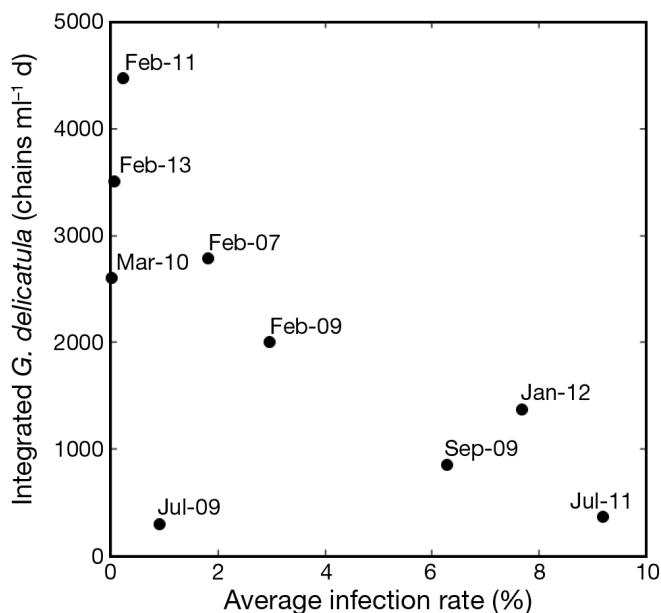


Fig. 5. Relationship between magnitude of *Guinardia delicatula* blooms (integrated abundance) and average infection rate ( $r = -0.67$ ,  $p = 0.025$ , considering all data points including summer 2009). Date labels indicate midpoint for each event by year and month. Blooms in 2008 were excluded due to data gaps during the events

sence of parasite-induced losses. In fact, our time series results are consistent with this hypothesis; winter periods with more evidence of parasite attack generally had reduced *G. delicatula* blooms (Figs. 2 & 5). Interestingly, this conclusion is similar to findings of Ibelings et al. (2011), who studied chytrid parasites of the diatom *Asterionella formosa* in a freshwater lake; in that system, they observed almost no infection at water temperatures <3°C, and corresponding evidence for boom–bust cycles of host and parasite only in years with cold winters or early spring periods.

Diatom blooms are expected to be influenced by a variety of processes, notably those that control availability of light and nutrients as they impact growth physiology and those that control interactions with predators of different types. For *G. delicatula*, in particular, extended time series studies in the North Sea have documented changes in bloom timing and duration that appear related in different ways to temperature, water transparency, nutrient concentrations, biomass of certain mesozooplankton, and potential size of an overwintering resting stage pool (Wiltshire et al. 2010, Schlüter et al. 2012). The net impact in that system, where *G. delicatula* blooms are typical in spring through fall, has been a multi-decade trend of increase in its contribution to the phytoplankton community. For New England Shelf waters, where *G. delicatula* occurs principally in winter, our results suggest that parasite presence is a major factor controlling blooms in recent years. We found a significant negative relationship between bloom magnitude and average infection rate during the event (Fig. 5). In our time series, the record warm winter of 2012 was the only one warm enough to allow the parasites to maintain consistent levels of infection throughout the winter; this year had a very small winter bloom more consistent with typical summer events. In contrast, the cold winters of 2011 and 2013 had very low parasite incidence and supported the largest *G. delicatula* blooms in the record, while the winters of 2007 and 2009 were intermediate in terms of both infection rate and bloom magnitude. A smaller bloom than might be predicted on the basis of parasite presence occurred in summer 2009, suggesting that some other factor must have limited the magnitude of that bloom. Notably, we observed no large-magnitude blooms unless infection rate was low. Considering all events except the summer 2009 bloom (outlier,  $p = 0.011$ ), infection rate explains 80% of the variance in bloom magnitude ( $r^2 = 0.80$ ,  $p = 0.001$ ). Future experimental and process studies are needed to address the ways that these kinds of infection impacts may interact with other types of biologi-



cal and ecological factors that influence *G. delicatula* both on the New England shelf and in other regions.

As in many ocean regions, our study area shows high interannual variability, but also a significant increasing trend in water temperatures over recent decades (Nixon et al. 2004). Looking forward as temperatures continue to rise, winter periods of water below 4°C will shorten or disappear. These factors suggest the possibility that parasite impacts on species such as *G. delicatula* may increase, with immediate impacts on their population dynamics. Longer time series that encompass more warm winters will be needed to evaluate this idea. If the pattern persists, ultimately, this could alter the diatom community structure in these temperate waters where *G. delicatula* is currently a major component of the phytoplankton.

**Acknowledgements.** This work was supported by grants from NSF's Ocean Technology and Interdisciplinary Coordination program, NASA's Ocean Biology and Biogeochemistry program and Biodiversity and Ecological Forecasting program, the Gordon and Betty Moore Foundation, and the National Ocean Partnership Program. We are indebted to the MVCO Operations Team, especially Janet Fredericks, Jay Sisson, and Hugh Popenoe, for their dedication and skill. Alexi Shalapyonok and Taylor Crockford provided excellent technical and logistical support, and Joe Futrelle enabled exceptional informatics solutions to the challenges of dealing with hundreds of millions of images.

#### LITERATURE CITED

- Austin T, Edson J, McGillis W, von Alt C and others (2000) The Martha's Vineyard Coastal Observatory: a long term facility for monitoring air-sea processes. Proc OCEANS 2000 MTS/IEEE Conference and Exhibition, Providence, RI, p 1937–1941
- Breiman L (2001) Random forests. *Mach Learn* 45:5–32
- Brosnahan ML, Farzan S, Keafer BA, Sosik HM, Olson RJ, Anderson DM (2013) Complexities of bloom dynamics in the toxic dinoflagellate *Alexandrium fundyense* revealed through DNA measurements by imaging flow cytometry coupled with species-specific rRNA probes. *Deep-Sea Res II*. doi:10.1016/j.dsr2.2013.05.034
- Brussaard CPD, Kuipers B, Veldhuis MJW (2005) A mesocosm study of *Phaeocystis globosa* population dynamics I. Regulatory role of viruses in bloom control. *Harmful Algae* 4:859–874
- Campbell L, Olson RJ, Sosik HM, Abraham A, Henrichs DW, Hyatt CJ, Buskey EJ (2010) First harmful *Dinophysis* (Dinophyceae, Dinophysiales) bloom in the U.S. is revealed by automated imaging flow cytometry. *J Phycol* 46:66–75
- Campbell L, Henrichs D, Olson R, Sosik H (2013) Continuous automated imaging-in-flow cytometry for detection and early warning of *Karenia brevis* blooms in the Gulf of Mexico. *Environ Sci Pollut Res Int* 20: 6896–6902
- Canter HM, Lund JWG (1948) Studies on plankton parasites. *New Phytol* 47:238–261
- Chambouvet A, Morin P, Marie D, Guillou L (2008) Control of toxic marine dinoflagellate blooms by serial parasitic killers. *Science* 322:1254–1257
- Coats DW, Park MG (2002) Parasitism of photosynthetic dinoflagellates by three strains of *Amoebophrya* (Dinophyta): parasite survival, infectivity, generation time, and host specificity. *J Phycol* 38:520–528
- Drebes G, Schnepf E (1982) Phagotrophy and development of *Paulsenella* cf. *chaetoceratis* (Dinophyta), an ectoparasite of the diatom *Streptotheca thamesis*. *Helgol Meeresunters* 35:501–515
- Drebes G, Schnepf E (1988) *Paulsenella chatton* (Dinophyta), ectoparasites of marine diatoms: development and taxonomy. *Helgol Meeresunters* 42:563–581
- Drebes G, Schnepf E (1998) *Gyrodinium undulans* Hulburt, a marine dinoflagellate feeding on the bloom-forming diatom *Odontella aurita*, and on copepod and rotifer eggs. *Helgol Meeresunters* 52:1–14
- Drebes G, Kühn SF, Gmelch A, Schnepf E (1996) *Cryothecomonas aestivalis* sp. nov., a colourless nanoflagellate feeding on the marine centric diatom *Guinardia delicatula* (Cleve) Hasle. *Helgol Meeresunters* 50:497–515
- Fredericks JJ, Trowbridge JH, Austin TC, Sosik HM, Olson RJ, Traykovski PA (2006) Martha's Vineyard Coastal Observatory: existing infrastructure for interdisciplinary science. Proc IEEE 4th International Workshop on Scientific Use of Submarine Cables and Related Technologies, Dublin
- Gachon CMM, Sime-Ngando T, Strittmatter M, Chambouvet A, Kim GH (2010) Algal diseases: spotlight on a black box. *Trends Plant Sci* 15:633–640
- Ibelings BW, Gsell AS, Mooij WM, Van Donk E, Van Den Wyngaert S, De Senerpont Domis LN (2011) Chytrid infections and diatom spring blooms: paradoxical effects of climate warming on fungal epidemics in lakes. *Freshw Biol* 56:754–766
- Kim D, Kim JF, Yim JH, Kwon SK, Lee CH, Lee HK (2008) Red to red—the marine bacterium *Hahella chejuensis* and its product prodigiosin for mitigation of harmful algal blooms. *J Microbiol Biotechnol* 18:1621–1629
- Kühn SF, Drebes G, Schnepf E (1996) Five new species of the nanoflagellate *Pirsonia* in the German Bight, North Sea, feeding on planktic diatoms. *Helgol Meeresunters* 50:205–222
- Menden-Deuer S, Lessard EJ (2000) Carbon to volume relationships for dinoflagellates, diatoms, and other protist plankton. *Limnol Oceanogr* 45:569–579
- Moberg EA, Sosik HM (2012) Distance maps to estimate cell volume from two-dimensional plankton images. *Limnol Oceanogr Methods* 10:278–288
- Montagnes DJS, Chambouvet A, Guillou L, Fenton A (2008) Responsibility of microzooplankton and parasite pressure for the demise of toxic dinoflagellate blooms. *Aquat Microb Ecol* 53:211–225
- Nixon S, Granger S, Buckley B, Lamont M, Rowell B (2004) A one hundred and seventeen year coastal water temperature record from Woods Hole, Massachusetts. *Estuaries* 27:397–404
- Olson RJ, Sosik HM (2007) A submersible imaging-in-flow instrument to analyze nano- and microplankton: Imaging FlowCytobot. *Limnol Oceanogr Methods* 5:195–203
- Olson RJ, Shalapyonok A, Sosik HM (2003) An automated submersible flow cytometer for analyzing pico- and nanophytoplankton: FlowCytobot. *Deep-Sea Res I* 50:301–315
- Park MG, Yih W, Coats DW (2004) Parasites and phyto-

- plankton, with special emphasis on dinoflagellate infections. *J Eukaryot Microbiol* 51:145–155
- Schlüter MH, Kraberg A, Wiltshire KH (2012) Long-term changes in the seasonality of selected diatoms related to grazers and environmental conditions. *J Sea Res* 67: 91–97
- Schnepf E, Drebes G, Elbrächter M (1990) *Pirsonia guinardiae*, gen. et spec. nov.: A parasitic flagellate on the marine diatom *Guinardia flaccida* with an unusual mode of food uptake. *Helgol Meeresunters* 44:275–293
- Scholin C, Jensen S, Roman B, Massion E and others (2006) The Environmental Sample Processor (ESP—An autonomous robotic device for detecting microorganisms remotely using molecular probe technology. *Proc OCEANS 2006*, Boston, MA, p 1–4
- Sieracki CK, Sieracki ME, Yentsch CS (1998) An imaging-in-flow system for automated analysis of marine microplankton. *Mar Ecol Prog Ser* 168:285–296
- Sime-Ngando T (2012) Phytoplankton chytridiomycosis: fungal parasites of phytoplankton and their imprints on the food web dynamics. *Front Microbiol* 3:361
- Sosik HM, Olson RJ (2007) Automated taxonomic classification of phytoplankton sampled with imaging-in-flow cytometry. *Limnol Oceanogr Methods* 5:204–216
- Sosik H, Olson R, Armbrust EV (2010) Flow cytometry in phytoplankton research. In: Suggest DJ, Prášil O, Borowitzka MA (eds) *Chlorophyll a fluorescence in aquatic sciences: methods and applications*, Book 4. Springer, Dordrecht, p 171–185
- Tillmann U, Hesse KJ, Tillmann A (1999) Large-scale parasitic infection of diatoms in the Northfrisian Wadden Sea. *J Sea Res* 42:255–261
- Van Donk E (1989) The role of fungal parasites in phytoplankton succession. In: Sommer U (ed) *Plankton ecology*. Springer, Berlin, p 171–194
- Wiltshire K, Kraberg A, Bartsch I, Boersma M and others (2010) Helgoland Roads, North Sea: 45 years of change. *Estuaries Coasts* 33:295–310

*Editorial responsibility: Toshi Nagata, Kashiwanoha, Japan*

*Submitted: November 27, 2013; Accepted: March 13, 2014  
Proofs received from author(s): April 7, 2014*